RSC Advances

ROYAL SOCIETY OF CHEMISTRY

www.rsc.org/advances

Journal Name

RSCPublishing

ARTICLE

Low temperature synthesis of rutile TiO_2 single-crystal nanorods with exposed (002) facets and its decoration of gold nanoparticles for photocatalytic application

Cite this: DOI: 10.1039/x0xx00000x

Received 00th January 2012,
Accepted 00th January 2012

DOI: 10.1039/x0xx00000x

www.rsc.org/

Lijuan Bu,[a] Wenjing Yang[c] and Hai Ming[b]*

Uniform rutile TiO_2 single crystal nanorods (TNRs) enclosed by high aspect of active (002) facets were synthesized by treating anatse TiO_2 with concentrated HNO_3 under hydrothermal condition for the first time. It was found that these TNRs exhibited considerably enhanced photocatalytic activity compared to bulk rutile TiO_2 owing to the highly exposed active (002) facets. Besides, gold nanoparticle with a diameter of 1-5 nm were successfully deposited on TNRs (Au/TNRs) using a simple photocatalytic reduction of $HAuCl_4$ by the TNRs in the presence of 2-Propanol. Plasmon-induced photocatalytic-chemistry of the Au/TNRs under ultraviolet and visible light was investigated. The photocatalytic ability of TNRs was obviously enhanced under ultraviolet light with the decoration of Au nanoparticles. Particularly, the Au/TNRs nanocomposite demonstrated much better photocatalytic ability under visible-light than that under the ultraviolet light in our experimental condition. This phenomenon may attribute to the intense localization of plasmonic near-fields close to the Au-TiO_2 interface, which brings about enhanced optical absorption and is good for generating electron-hole pairs for photocatalysis.

Introduction

Synthesis of micro-particles and nano-crystals with exposed high-energy or active facets (*e.g.*, Pt, Au, TiO_2, V_2O_5, ZnO, Fe_3O_4, WO_3) have attracted a great deal attention because they usually exhibit fascinating interfacial behaviours and were applied in many fields including catalysis, sensor, photovoltaic, environmental and energy storage.[1-5] Up to now, TiO_2 has been proven to be one of the most versatile material among various oxide in photo-catalysis, paint, sensor devices and rechargeable battery applications benefiting from its impressive semiconductor properties, low cost, robust crystal structure and excellent stability. As a result, researches concerning morphology, size, surface and crystal structures of TiO_2 are being intensively explored.[6] For example, the order of the average surface energies of anatase TiO_2 was proved to be 0.90 J m^{-2} for (001) > 0.53 J m^{-2} for (100) > 0.44 J m^{-2} for (101),[7] and the meta-stable (001) facets of anatase have a positive effect on the photocatalytic ability under the ultraviolet (UV) or visible (Vis) light. Particularly, numerous works aiming to TiO_2 anatase with dominant facet were developed worldwide since the pioneering work by Yang *et al.*[8,9]

In addition, decoration of noble metal particles (*e.g.*, Au, Pt, Pd, Ru) on certain substrate of metal (oxides), carbon, or polymer is good for pursuing higher performance in many photo-induced reactions.[10] Especially, the use of Au nanoparticles (NPs) was confirmed to be extremely effective in promoting photocatalytic reactions within a wide range of light spectra because the surface plasmon resonance (SPR) effect from Au NPs can be excited by Vis light illumination.[10] And also, interfacial loading of AuNPs on TiO_2 could largely increase the migration of photoelectrons, so as to promote the separation of electrons and holes, thereby playing an important role to enhance its photocatalytic activity.[10,11] Therefore, the composite of Au/TiO_2 has a great potential applications in photocatalytic reactions. As mentioned, the interfacial properties of TiO_2 single crystals is crucial to determine its stability and reactivity and also affect the loading of AuNPs. High-energy surface atoms exhibit high activity and are easy to combine with the foreign atoms such as the Au atoms to form a stable structure.[12] Hence, preparing TiO_2 single crystals with exposed high-energy facets loaded with Au NPs was always interest to get certain specific photocatalytic behaviors, as proved by Gong *et al.*. They found that the exposed active (001) and (110) facets of TiO_2 loaded with Au NPs dramatically enhanced the UV light photocatalytic performance.[13] Considering the more thermodynamical stability of rutile TiO_2 than the anatase with little lower direct band gap (~3.0 eV *vs.* 3.2 eV of anatase),[14] it would be considerably attractive to load Au NPs on rutile TiO_2 single

crystals with highly exposed facets and investigate its phohocatalytic ability for enriching the fundamental study and getting a better understanding the synergetic behaviours between the Au and TiO_2.

Although considerable efforts have been devoted to the synthesis and applications of hierarchical structures consisting of anatase or rutile nanocrystals with dominant facets, scarcely any successful method achieved on the preparation of rutile crystals with a large percentage of (002) facets in scalable production. In this work, a new kind rutile TiO_2 single crystal nanorods with highly exposed (002) facets was introduced and prepared readily by treating anatse TiO_2 with concentrated HNO_3 under a mild hydrothermal condition for the first time. The TNRs exhibited considerably enhanced photocatalytic activity compared to bulk rutile TiO_2 owing to its highly exposed active (002) facets. Furthermore, ultra-small AuNPs (1~5 nm) were successfully deposited on TNRs (i.e., Au/TNRs), and then plasmon-induced photocatalytic-chemistry of Au/TNRs in the UV and Vis region was studied. Compared to bare TNRs, the photocatalytic ability of Au/TNRs was obviously enhanced under UV light. More interestingly, Au/TNRs hybrids exhibited a much better Vis-light photocatalytic performance than that under UV light in our experimental condition. This phenomenon may benefit from the intense localization of plasmonic near-fields close to the Au-TiO_2 interface, which could bring about enhanced optical absorption and facilitate the generation of electron-hole pairs.

Experimental Section

Preparation of anatase TiO_2 nanoparticles

All chemicals were used as received without further purification. Typically, 4 mLTetra-n-butyl Titanate (purchased from Alfa Aesar Co. Ltd., named as TBT) were dissolved into 100 mL ultra-pure ethanol. On the other hand, a certain amount of HCl was added into 200 mL H_2O to adjust the pH value around 1, and then it was transferred to a 500 mL three-neck flask and heated at 343 K in the oil bath. Above ethanol solution of TBT was dropped into the solution of HCl-H_2O with the rate of 1 ml min^{-1} under vigorous stirring to promote the hydrolysis of TBT, under which a white colloid solution was formed. Filtrate the solution and wash the product by ethanol and water for several times. Finally, the as-prepared white powders were dried at 343 K for 48 h.

Formation of the rutile TNRs

As-prepared TiO_2 nanoparticles were dispersed in concentrated HNO_3 (i.e., 69 wt.%) with a concentration of 10 mg ml^{-1}, and then the colloid was transferred into Teflon lined stainless steel autoclaves maintaining at 453 K for 24 h. After the autoclaves cool down to room temperature, a white suspension was obtained. The products was collected by centrifugation at 12000 rpm for 20 min and washed by ethanol and water several times, giving rise to highly crystallized TNRs.

Preparation of Au/TNRs nanocomposite

Typically, 0.18 g as-prepared TNRs or P25, modified with 3-mercaptopropionic acid and then dispersed in the solution of H_2O/2-propanol (IPA) (20 ml/5 ml), and then 4.5 ml of 25 mM $HAuCl_4$ aqueous solution was added. After that, the mixed solution was transferred into one-neck quartz flask and stirred violently for 4 h. Finally, this suspension was exposed to the UV light and stirred for 12 h, and finally Au/TNRs or Au/P25 nanohybrids were obtained after the centrifugation.

Photocatalytic activities and photoelectrochemical test

The photocatalytic activity of bulk rutile TiO_2, P25, TNRs, Au/P25, and Au/TNRs were evaluated by the degradation of rhodamine B (RhB) in aqueous solution. In a typical procedure, 50 mg TNRs, P25 or Au/TNRs was dispersed firstly into 100 mL RhB (10 ppm) separately, and then the suspension was kept stirring and irradiated by UV lamp-Spectroline SB-100P/F (100 W, λ: 50~400 nm) or a tungsten-halogen (100 W, λ:400~2500 nm) with an UV cut-off filter ($\lambda \geq 400$ nm). A cooling fan was used to avoid the increase of temperature in reaction system during irradiation. Before irradiation, the aqueous solution was magnetically stirred in dark for 12 h to reach the adsorption equilibrium of dye on catalyst surface, the absorption plots (Fig. S1) of RhB on different photocatalysts illuminated that the adsorption equilibrium is near stable after 12 h. Comparing to the pristine concentration of RhB (10 ppm), the absorption amount of these photocatalysts are about 10.2%-21.5% of the total pollutant (RhB). The adsorption capability of P25, TNRs, and bulk rutile TiO_2 decreased successively, which might agree with their decreased specific surface area. And also, the adsorption ability of Au/P25 and Au/TNRs were little lower than pristine one due to the decoration of Au particles. After initiation of irradiation, each 5 mL suspension was taken out at regular intervals of 10 or 30 min and then centrifuged to remove the catalyst completely. UV-Vis absorption spectra of the centrifuged solution were recorded using a spectrophotometer.

Measurement and characterization

X-ray powder diffraction (XRD) was obtained by using aX'Pert-ProMPD (Holand) D/max-γA X-ray diffractometer with Cu Kα radiation (λ=0.154178 nm). Transmission electron micrographs (TEM) and high-resolution TEM (HRTEM) were taken on a FEI-Tecnai F20 (200 kV) transmission electron microscope (FEI). Room temperature Solid UV-vis diffuse reflectance absorption spectra (UVDRS) was recorded on a Lambda 750 (PerkingElmer) spectrophotometer in the wavelength range of 200-800 nm.

Results and discussion

Nanostructure of TNRs

As shown in XRD patterns (Fig. 1a), the crystalline structure of TNRs (red curve) sample was classified to rutile phase (JCPDS: 87-0710). The intensity of characteristic peak at 62.79°, corresponding to the (002) crystal facets, is much higher than that of normal rutile TiO_2 indicating the highly exposed (002)

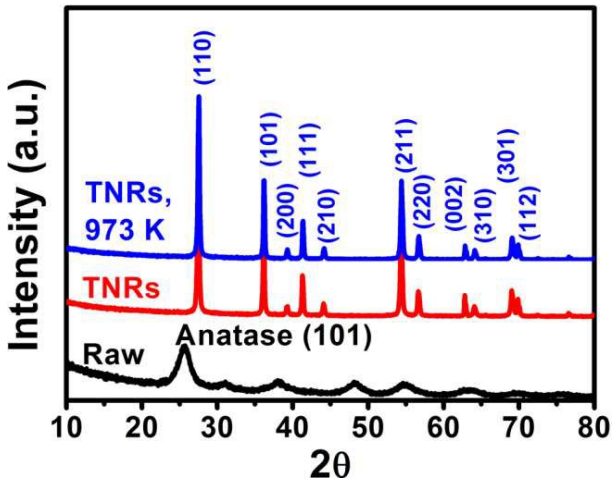

Fig. 1 XRD patterns of raw anatase, TNRs and TNRs after calcination at 973 K.

facets. Thermal treated the TNRs at 973K, its crystal phase well maintained and there is no obvious change, confirming the good stability and highly crystallinity of pristine TNRs synthesized in mild hydrothermal conditions. Before the hydrothermal treatment, raw materials are mainly composed of anatase (black curve), and the XRD results well show that the anatase crystalline TiO_2 can transform to rutile TiO_2 just through a simple acid hydrothermal strategy at a low temperature of 453 K.

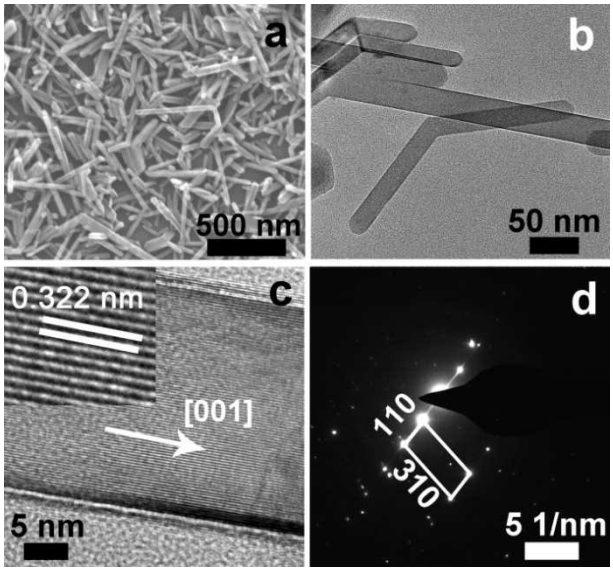

Fig. 2 (a) SEM, (b) TEM, (c) HRTEM, (d) SAED pattern of TNRs.

The high magnification SEM image of TNRs shows that their morphology were uniform nanorods with a diameter of 20-50 nm and length of 100-1000 nm (Fig. 2a), as further characterized by the TEM (Fig. 2b). They have very thin structure and smooth surface. The lattice fringes with lattice space of 0.322 nm along the [001] direction were clearly observed under HRTEM (Fig. 2c). Further, the well-separated diffraction spots in selected area electron diffraction (SAED) pattern fully illuminate the single-crystalline nature of TNRs, and the distance of light spots are 0.322 nm and 0.148 nm, corresponding to the facets of (110) and (310) respectively (Fig. 2d); meanwhile the angle between the (110) and (310) is about 28.3°, which is identical to the theoretical value between the {110} and {310} facets. These information confirm that the TNRs nanocrystals mainly expose {002}surfaces.[15]

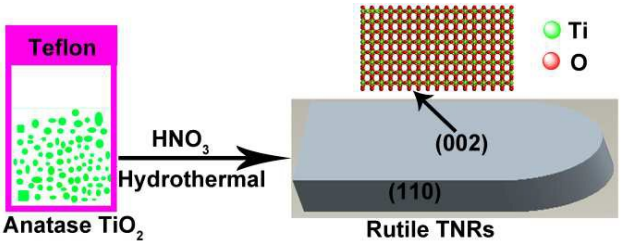

Fig. 3 Schematic drawing of the formation of TNRs.

Based on the crystalline structure of TNRs, a possible conversion mechanism was presented (Fig. 3). As we know, the different polymorphs of anatase, rutile, and/or brookite can be induced by local pH variations or relative complexation effect. In TiO_2, rutile crystalline structure is based on linear chains of TiO_6 octahedra by sharing equatorial edges, whereas anatase is based on a spiral chain of apical edge sharing TiO_6 octahedra.[16] Firstly in the hydrothermal process at 453 K, the anatase precursor may bond with the anionic ions of NO_3^- to form a anionic matrix $TiO_{2-x/2}[NO_3^-]_x[OH_2]_{x/2}$. Next, with the rising of temperature and pressure, the value of x will increase and the $TiO_{2-x/2}[NO_3^-]_x[OH_2]_{x/2}$ will further dehydrate due to the strong acidic medium. Additionally, the anion of NO_3^- will decompose in this critical conditions, while $TiO_{2-x/2}[NO_3^-]_x[OH_2]_{x/2}$ transfers to octahedral monomer ($[TiO(OH_2)_5]_2$) in strong acidic solution.[17] In the interfacial region of confined meso-structure, a linear chain arrangement of $[TiO(OH_2)_5]_2$ octahedral monomers (i.e., rutile nuclei) by sharing equatorial edges may be more favorable, rather than an apical edge sharing spiral structures (i.e., anatase nuclei) due to the geometric confinement.[18] In this way, lamellar rutile nanocrystals grow along the [001] direction. The interfacial charge density of TiO_2 decreases due to the elimination of positive charges in the TiO_2 framework, and then the two-dimensional lamellar rutile nanocrystals transforms into rutile nanorods. Particularly, a high pressure in thermal treatment and a supercritical state were good for forming highly crystallized TiO_2.

Nanostructure of Au/TNRs

Since TNRs has a special single crystalline structure similar to the monocrystal Si wafer and mica plate, it could be a good substrate processing for a photocatalytic mechanism research.

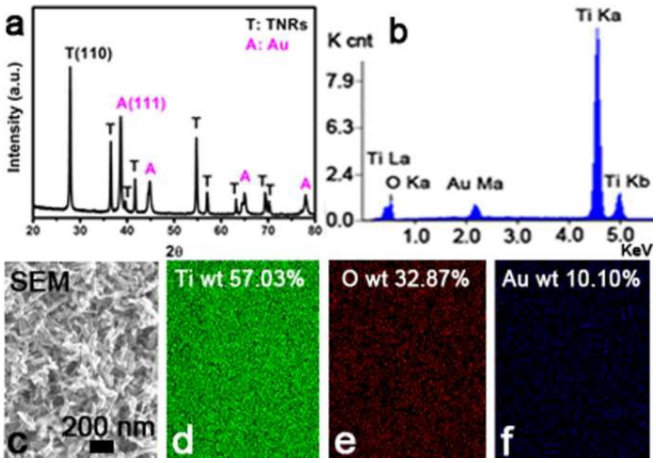

Fig. 4 (a) XRD pattern, (b) EDX spectrum, (c) SEM images and (d-f) EDS mappings of Au/TNRs.

To verify this, Au/TNRs nano-composites was prepared and their structure, physical and photocatalytic properties were investigated in detail, which are significant to enrich the knowledge of the AuNPs effect on the photocatalytic properties of TiO_2. Except the XRD peaks of TiO_2, other four peaks corresponding to the index of Au (111), (200), (220) and (311) appeared (Fig. 4a), directly demonstrating the existence of Au. It was further confirmed by the EDX spectrum of Au/TNRs containing the Ti, Au and O elements (Fig. 4b). Further as demonstrated by the SEM image and EDS-mapping, the mass ratio of Au is about 10.1 wt% with a very uniform distribution (Fig. 4c-f).

The AuNPs distribution on TNRs was further demonstrated by TEM images. As shown in Fig. 5a-b, TNRs

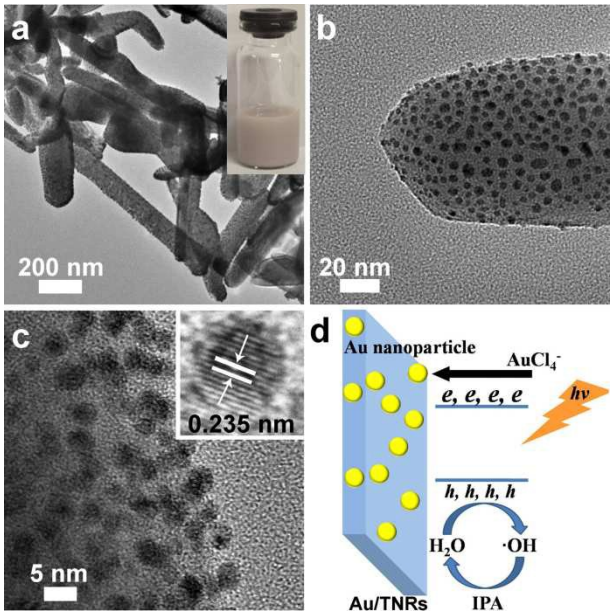

Fig. 5 (a, b) TEM and (c) HRTEM images of Au/TNRs; (d) Scheme for the formation of Au/TNRs.

were uniformly decorated with plenty of AuNPs around the size of 1-5 nm. The close-knit of AuNPs and one dimensional TNRs in junction structures indicate their nice combine after UV irradiation treatment. The fine and well-resolved lattice fringe of black dots exhibit an inter-planar distance of 0.235 nm, corresponding to the Au (111) plane well. The digital photo of Au/TNRs solution has a typical white-purple color (inset of Fig. 5a). The reason of close-knit of AuNPs and TNRs may ascribe to the ingenious design of experiment (Fig. 5d). Firstly, irradiation of TNRs by UV light can produce a lot of electrons and holes due to the narrow band gap of 3.0 eV sensitive to the UV light. Once the $AuCl_4^-$ contacts with TNRs surface in solution, the Au(III) could be in-situ reduced to Au(0) atom and closely link with TNRs due to the low polarization and surface tension of IPA/H_2O solution. Accompanying the deposition of Au(0) on TNRs, the site of Au(0)/TNRs could produce more electrons around the surface of Au(0) nuclei and then further facilitate its grow. Besides, the IPA is a hole trapping agent, and it could sufficiently separate the electron and hole in Au/TNRs(0), which could continually reduce the Au(III) and keep the regular growth of AuNPs.[19] Finally, the AuNPs can combine with TNRs tightly. However, for the sample P25, the particle size of loaded Au on P25 was as large as 10-30 nm and not uniform (Fig. S2). The reason should be ascribed to the short of high energy crystal surface of P25 for loading the Au nuclei and a fast grow of Au particles under the UV irradiation on P25.[13]

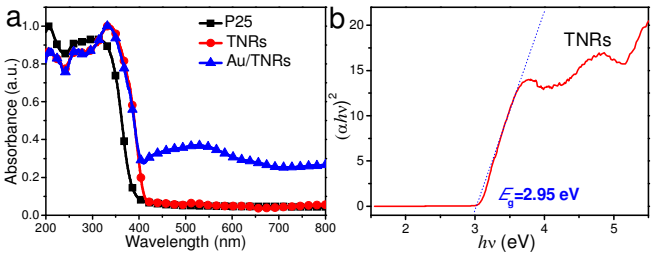

Fig. 6 (a) UVDRS spectra of the TNRs, Au/TNRs, and P25; (b) Indirect inter band transition energy of the TNRs.

UV-vis diffuse reflectance spectroscopy (UVDRS) was used to characterize the electronic states (Fig. 6a), and it indicate that the band gap absorption onset of P25 and TNRs located around 380 nm (black curve) and 420 nm (red curve), respectively, while Au/TNRs show an efficient absorption in Vis-range of 420-800 nm, implying a good photocatalytic ability of Au/TNRs under Vis light. The UVDRS of pristine TNRs exhibits a broad absorption band from 200 to 420 nm, thus the band gap energy of this sample can be calculated by using $(\alpha hv)^n = k(hv\text{-}E_g)$, where α is the absorption coefficient, k is the parameter that related to the effective masses associated with the valence and conduction bands, n is 2 for a direct transition, hv is the absorption energy, and E_g is the band gap energy. Plotting $(\alpha hv)^2$ *vs.*hv based on the spectral response gives the extrapolated intercept corresponding to the E_g value (Fig. 6b). The optical band energy of the rutile TNRs is 2.95 eV, which exhibits a slight red-shift of 0.05 eV with respect to 3.0 eV of

normal rutile TiO_2. This phenomenon is acceptable, because changes of crystal structure and morphology could affect the optical properties.[14,20,21]

Photocatalytic Properties of TNRs and Au/TNRs

To investigate the photocatalytic activity of Au/TNRs, photo-degradation of RhB under the UV light (λ: 50~400 nm) and Vis light (λ: 400~2500 nm) were performed compare to the catalyst of TNRs, P25, and Au/P25. As shown in Fig. 7a, irradiated with UV light, 10 ppm of RhB can be degraded completely by P25 and Au/P25 within 80 min because of their double crystalline phase of anatase/rutile; while the degradative amount of RhB were only 28%, 45% and 58% for the bulk rutile TiO_2, TNRs and Au/TNRs respectively even prolong the irradiation time to 120 min. The TNRs exhibited improved catalytic ability compare to bulk rutile TiO_2 owing to the dominant active (002) facets, and also the introduction of AuNPs on TNRs give rise to higher catalytic activity than pristine TNRs.

This phenomena could be interpreted from the reaction mechanism, and generally the photocatalytic pathway in Au/semiconductor could be summarized as follows: semiconductor adsorbs photons and excites electrons from the valence band to the conduction band, creating highly reactive electron and hole pairs. Some of the pairs recombine while some migrate towards the semiconductor surface to be involved in the photocatalytic reaction. The electrons may be trapped by oxygen to form oxygen species ($\cdot O_2^-$).[22] The photo-generated holes may be trapped by hydroxyl groups attached on the surface to form hydroxyl radicals (·OH).[23] These hydroxyl radicals and oxygen species oxidize the RhB into carbon dioxide, water and some simple mineral acids in aqueous solution. While for the sample of Au/TNRs, the photoelectrons can be captured by gold particles and subsequently transferred to the adsorbed O_2, leading to the effective separation of electrons and holes and then available to increase the photocatalytic activity.[24]

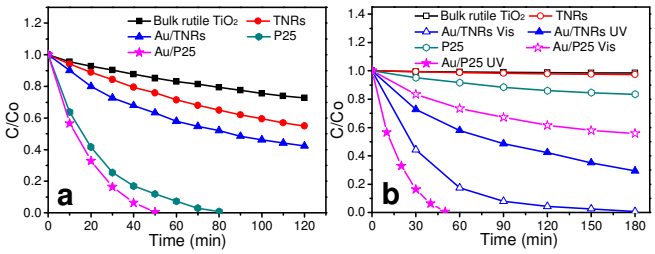

Fig. 7 Comparison of (a) UV and (b) Vis-driven photocatalytic activity of the bulk rutile TiO_2, pure TNRs, Au/TNRs, P25,and Au/P25 for photodegradation of RhB, C_0 is the relative concentration of the RhB in solution after balancing absorption.

Further, more interesting and entirely different results were collected in reaction system irradiated by tungsten-halogen with an UV cut-off filter (λ≥ 400 nm) (Fig. 7b). The Au/TNRs are able to degrade RhB completely within 3 hours, while the residual amount of RhB for bulk rutile TiO_2, P25, TNRs, and Au/P25 are as high as 98.5%, 97.4%, 87.6% and 55.8%. Moreover, the catalyst of Au/TNRs demonstrate a high cycle ability in initial 10 cycles and was available to fully degrade RhB within 3 hours (Fig. S3). It has a better catalytic ability under the Vis light than that under the UV light when both light powers keep the same, while this phenomenon is completely inverse for the sample of Au/P25. The impressive catalytic behavior of Au/TNRs may relative to their special electronic system, and various enhancement mechanisms could be proposed, such as SPR-mediated charge injection from metal to semiconductor and plasmonic heating. In the SPR-mediated charge injection mechanism, the plasmonic AuNPs behave like a light absorber, and charge carries generated from the excited AuNPs will be directly injected into the adjacent TiO_2, in a manner analogous to dye sensitization.[25] In which, the photoreactions take place at the phase boundaries of metal-semiconductor-liquid. Under this condition, once excited by SPR, the electrons would move from AuNPs to the conduction band of TiO_2 and then drive the reduction reaction of RhB. Another mechanism was also put forward to explain plasmonic effect when the plasmonic AuNPs are in direct contact with TiO_2. SPR is able to enhance the local electric fields in the vicinity of the AuNPs, and the interaction of local electric fields with the proximate TiO_2 allows the facile generation of electron-hole pairs in the interfacial area of the Au-TiO_2.[26] In this case, the photoreaction centres are at metal-semiconductor-liquid three phase boundaries, and they spread away from the three phase boundaries along the semiconductor-liquid interface. Yet the UVDRS spectra of TNRs and Au/TNRs indicate that TNRs is not sensitive to the Vis light, thus this plasmonic heating mechanism should not be the main factor to the enhanced photocatalytic performance of the Au/TNRs.

No matter which reaction mechanism, all photoreactions occurred between/near the interface of TiO_2 and AuNPs, which are responsible for the better photocatalytic ability under the Vis light than that of UV. Once the plasmonic AuNPs were excited by Vis light and acted as the role of light harvester, AuNPs can absorb photons immediately and the charge carriers could be directly injected into adjacent TiO_2 conduction band, thereby fast separating the positive holes and negative electrons on AuNPs and TiO_2 conduction band respectively. This promotion effect could be further strengthened due to the close interaction of AuNPs and (002) facets of TNRs, in which a strong thermoelectric effect could be induced by SPR effect on high energy crystal facets and then further improve the transfer ability of photons. Meanwhile, AuNPs can introduce a very strong local electric field to the proximate TiO_2 matrix because of SPR and/or plasmon assisted Forster resonant energy transfer. Electron-hole pair could be formed in the strong local electric field even though the excitation energy of Vis-light is lower than the band gap of TiO_2 and the strong electric field of plasmonic AuNPs could effectively suppress the recombination of hole and electron. After separation, electron will transport to the surface of AuNPs to drive the generation of $\bullet O_2^-$, and hole will transport to the semiconductor/liquid surface and be captured by OH in liquid phase to form ·OH. Therefore, all these active species mainly distributed on the interface of TNRs and AuNPs, and then contact with pollutant sufficiently

towards an efficient degradation. Moreover, according to the effects of Au particle size in previous literatures (Table S1), an appropriate size below 12 nm is good for high performance; therefore, it is convinced that the AuNPs around 1-5 nm on Au/TNRs could play a positive role in improving the catalytic activity. However, in the case of Au/P25 irradiated by Vis light, it showed a better UV photocatalytic ability, and the reasons should be ascribed to the lack of (002) facets and larger Au particles with a wide distribution (Fig. S1), on which insufficient interfaces (metal-semiconductor-liquid) could be used to accelerate the photoreactions.[27,28] Besides, photodeposition of large Au particles can mask or block TiO_2 active sites and then lead to a decreased catalytic activity.[29-31]

In addition, possible reasons interpreting the low photocatalytic efficiency of Au/TNRs under UV irradiation was also discussed. Firstly, under the irradiation of Au/TNRs by UV, there is no SPR effect on nano-structured noble metal (*e.g.*, AuNPs), because SPR effect was mainly excited by Vis light illumination.[32,33] Secondly, the higher loading AuNPs around 10.1 % is much higher than the optimized amount below 2% in previous reports.[34,35] Excess AuNPs covered on TiO_2 surface may be the recombination centres for electrons and holes, thereby leading to the decrease of photocatalytic activity.[30,36] Thirdly, according to the formula of $E = Wt = nh/\lambda$ (where *W, t, n, h and* λ are the light power, irradiation time, number of photons, Planck constant and wavelength respectively), more number of photons could be obtained per unit time for Vis light ($\lambda \geq 400$ nm) comparing to those of UV light ($\lambda < 400$ nm) under the same light power, and it demonstrated that higher density of photos was introduced into the per unit volume of photoreaction system under the Vis irradiation. In other words, more Vis photos could be supplied by Vis irradiation even the trapping efficiency of Vis photos was little lower than that of UV, and then give rise to higher catalytic ability.

Conclusions

In summary, a new uniform rutile TiO_2 single crystal nanorods (TNRs) enclosed by high aspect of active (002) facets were synthesized just through treating anatse TiO_2 with concentrated HNO_3 at mild hydrothermal condition, and a possible conversion mechanism was presented preliminarily. As-prepared TNRs demonstrated considerably enhanced photocatalytic activity over bulk rutile TiO_2 and it may benefit from the dominant active (002) facets. Furthermore, a very uniform Au nanoparticle with the size of 1-5 nm were successfully deposited on TNRs (i.e., Au/TNRs) by photocatalytic reduction of $HAuCl_4$ on TNRs in the presence of 2-Propanol. In addition, plasmon-induced photocatalytic performance of Au/TNRs in the UV and Vis region was studied well compare to the catalyst of pristine TNRs, P25 and Au/P25. With the decoration of AuNPs, not only the catalytic ability of Au/TNRs was obviously enhanced in photo-degradation of RhB, but also the interesting results of better photocatalytic performance under Vis-light than that under UV light was found and investigated. This phenomenon discussed from the reaction mechanism and it may relative to the intense localization of plasmonic near-fields close to the interface of Au/TiO_2, which would bring enhanced optical absorption and facilitate the generation of electron-hole pairs for photocatalysis.

Acknowledgements

Financial supports from the Nature Science Foundation of China (Nos. 20873089, 20975073), Nature Science Foundation of Jiangsu Province (Nos. BK2011272), Industry-Academia Cooperation Innovation Fund Projects of Jiangsu Province (Nos. BY2011130), Project of Scientific and Technologic Infrastructure of Suzhou (SZS201207), Graduate Research and Innovation Projects in Jiangsu Province (CXZZ13_0802)and Hunan Provincial Innovation Foundation For Postgraduate (CX2012B206)are gratefully acknowledged.

Notes and references

[a]Key Laboratory of Chemical Biology and Traditional Chinese Medicine Research (Ministry of Education), College of Chemistry and Chemical Engineering, Hunan Normal University, Changsha 410081, P.R. China.
[b]College of Chemistry, Chemical Engineering and Materials Science, Soochow University, Suzhou 215123, P. R. China; E-mail: lunaticmh@163.com.
[c]Reliability Research and Analysis Center, CEPREI (East China) Laboratories, The Fifth Research Institute of MIIT East China, P. R. China.

† Footnotes should appear here. These might include comments relevant to but not central to the matter under discussion, limited experimental and spectral data, and crystallographic data.

Electronic Supplementary Information (ESI) available: [details of any supplementary information available should be included here]. See DOI: 10.1039/b000000x/

1 T. L. Thompson and J. T. Yates, *Chem. Rev.,* 2006, **106**, 4428-4453
2 H. Tada, T. Kiyonaga and S. Naya, *Chem. Soc. Rev.,* 2009, **38**, 1849-1858
3 M. D'Arienzo, J. Carbajo, A. Bahamonde, M. Crippa, S. Polizzi, R. Scotti, L. Wahba and F. Morazzoni, *J. Am. Chem. Soc.,* 2011, **133**, 17652-61
4 C. J. Jia, L. D. Sun, F. Luo, X. D. Han, L. J. Heyderman, Z. G. Yan, C. H. Yan, K. Zheng, Z. Zhang, M. Takano, N. Hayashi, M. Eltschka , M. Kläui, U. Rüdiger, T. Kasama, L. Cervera-Gontard, R. E. Dunin-Borkowski, G. Tzvetkov and J. Raabe, *J. Am. Chem. Soc.,* 2008, **130**, 16968-16977.
5 G. Liu, H. G. Yang, X. W. Wang, L. N. Cheng, J. Pan, G. Q. Lu and H. M. Cheng, *J. Am. Chem. Soc.,* 2009, **131**, 12868-12869.
6 M. Lazzeri, A. Vittadini and A. Selloni, *Phys. Rev. B.,* 2001, **63**, 155409.
7 U. Diebold, *Surf. Sci. Rep.,* 2003, **48**, 53.
8 H. G. Yang, C. H. Sun, S. Z. Qiao, J. Zou, G. Liu, S. C. Smith, H. M. Cheng and G. Q. Lu, *Nature,* 2008, **453**, 638-641.
9 X. W. Zhao, W. Z. Jin, J. G. Cai, J. F. Ye, Z. H. Li, Y. R. Ma, J. L. Xie and L. M. Qi, *Adv. Funct. Mater.,* 2011, **21**, 3554-3563.
10 S. Y. Zhu, S. J. Liang, Q. Gu, L. Y. Xie, J. X. Wang, Z. X. Ding and P. Liu, *Appl. Catal. B-Eeviron.*, 2012, **119-120**, 146-155; M. Murdoch, G. I. N. Waterhouse, M. A. Nadeem, J. B. Metson, M. A. Keane, R. F. Howe, J. Llorca and H. Idriss, *Nat. Chem.,* 2011, **3**, 489-492; X. M. Zhang, Y. L. Chen, R.-S. Liu and D. P.Tsai, *Rep. Prog. Phys.,* 2013, **76**, 046401.

11 X. Zhang, Y. Liu, S. T. Lee, S. H. Yang and Z. H. Kang, *Energy Environ. Sci.,* 2014, **7**, 1409-1419.
12 X. Q. Gong, A. Selloni, O. Dulub, P. Jacobson and U. Diebold, *J. Am. Chem. Soc.,* 2008, **130**, 370-381.
13 M. Y. Xing, B. X. Yang, H. Yu, B. Z. Tian, S. Bagwasi, J. L. Zhang and X. Q. Gong, *J. Phys. Chem. Lett.,* 2013, **4**, 3910-3917. R. G. Li, H. X. Han, F. X. Zhang, D. G. Wang and C. Li, *Energy Environ. Sci.,* 2014, **7**, 1369-1376.
14 E. Bae and T. Ohno, *Appl. Catal. B-Eeviron.,* 2009, **91**, 634-639.
15 S. W. Liu, J. G. Yu and M. Jaroniec, *Chem. Mater.,* 2011, **23**, 4085-4093.
16 Y. Q. Zheng, E. R. Shi, Z. Z. Chen, W. J. Li and X. F. Hu, *J. Mater. Chem.,* 2001, **11**, 1547-1551; S. Cassaignon, M. Koelsch and J. P. Jolivet, *J. Phys. Chem. Solids*, 2007, **68**, 695-700; A. Pottier, C. Chaneac, E. Tronc, L. Mazerolles and J. P. Jolivet, *J. Mater. Chem.,* 2001, **11**, 1116-1121.
17 F. P. Rotzinger and M. Graetzel, *Inorg. Chem.*, 1987, **26**, 3704-3708.
18 Y. Z. Li, N. H. Lee, D. S. Hwang, J. S. Song, E. G. Lee and S. J. Kim, *Langmuir,* 2004, **20**, 10838-10844.
19 H. Ming, H. Huang, K. M. Pan, H. T. Li, Y. Liu and Z. H. Kang, *J. Solid State Chem.,* 2012, **192**, 305-311.
20 D. Q. Zhang, G. S. Li, F. Wang and J. C. Yu, *CrystEngComm,* 2010, **12**, 1759-1763
21 K. S. Lee and M. A. EI-Sayed, *J. Phys. Chem. B,* 2005, **109**, 20331-20338.
22 A. Furube, L. C. Du, K. Hara, R. Katoh and M. Tachiya, *J. Am. Chem. Soc.,* 2007, **129**, 14852-14853.
23 M. Teranishi, S. Naya and H. Tada, *J. Am. Chem. Soc.,* 2010, **132**, 7850-7851.
24 J. D. Stiehl, T. S. Kim, S. M. McClure and C. B. Mullins, *J. Am. Chem. Soc.,* 2004, **126**, 1606-1607.
25 Y. Tian and T. Tatsuma, *J. Am. Chem. Soc.,* 2005, **127**, 7632-7637.
26 I. Thomann, B. A. Pinaud, Z. B. Chen, B. M. Clemens, T. F. Jaramillo and M. L. Brongersma, *Nano Lett.,* 2011, **11**, 3440-3446.
27 J. Li and H. C. Zeng, *Chem. Mater.,* 2006, **18**, 4270-4277.
28 S. H. Overbury, V. Schwartz, D. R. Mullins, W. F. Yan and S. Dai, *J. Catal.,* 2006, **241**, 56-65.
29 B. Z. Tian, J. L. Zhang, T. Z. Tong and F. Chen, *Appl. Catal. B: Environ.,* 2008, **79**, 394-401.
30 M. C. Hidalgo, J. J. Murcia, J. A. Navío and G. Colón, *Appl. Catal. A: Gen.,* 2011, **397**, 112-120.
31 B. Cojocaru, Ş. Neaţu, E. Sacaliuc-Pârvulescu, F. Lévy, V. I. Pârvulescu and H. Garci, *Appl. Catal. B: Environ.,* 2011, **107**, 140-149.
32 Z. Y. Zhan, J. N. An, H. C. Zhang, R. V. Hansen and L. X. Zheng, *ACS Appl. Mater. Interfaces,* 2014, **6**, 1139-1144.
33 S. Sarina, E. R. Waclawik and H. Y. Zhu, *Green Chem.,* 2013, **15**, 1814-1833.
34 A. Ayati, A. Ahmadpour, F. F. Bamoharram, B. Tanhaei, M. Mänttäri, and M. Sillanpää, *Chemosphere,* 2014, **107**, 163-174.
35 R. Kaur and B. Pal, *J. Mol. Catal. A: Chem.,* 2012, **355**, 39-43.
36 B. Tian, C. Li, F. Gu and H. Jiang, *Catal. Commun.,* 2009, **10**, 925-929.

Graphic abstract

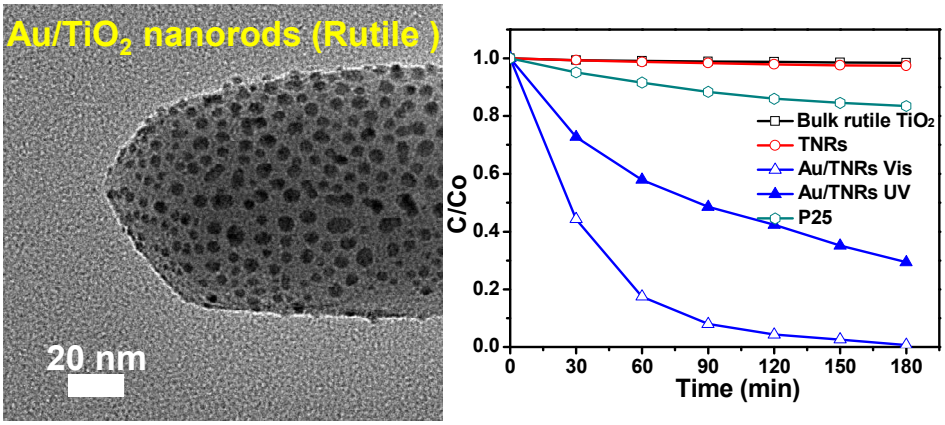

TiO_2 single crystal nanorods (TNRs) with dominant (002) facets and its derivate Au/TNRs were prepared and investigated in photocatalytic reaction.